

1 **Seasonal Forecasts of Winter Temperature Improved by**
2 **Higher-Order Modes of Mean Sea Level Pressure**
3 **Variability in the North Atlantic Sector**

4 **Clementine Dalelane, Mikhail Dobrynin, Kristina Fröhlich**

5 Deutscher Wetterdienst (DWD)

6 **Key Points:**

- 7 • The hybrid seasonal forecast combines a dynamical forecast ensemble and a sta-
8 tistical prediction of general atmospheric circulation indices
- 9 • Dynamical seasonal forecasts are subsampled with respect to four statistically pre-
10 dicted circulation indices in the North Atlantic sector
- 11 • Forecast skill of sea level pressure, surface temperature and precipitation is im-
12 proved across Europe compared to ensemble mean forecasts

Corresponding author: Clementine Dalelane, clementine.dalelane@dwd.de

Abstract

The variability of the sea level pressure in the North Atlantic sector is the most important driver of weather and climate in Europe. The main mode of this variability, the North Atlantic Oscillation (NAO), explains up to 50% of the total variance. Other modes, known as the Scandinavian index, East Atlantic and East Atlantic/West Russian pattern, complement the variability of the sea level pressure, thereby influencing the European climate. It has been shown previously that a seasonal prediction system with enhanced winter NAO skill due to ensemble subsampling entails an improved prediction of the surface climate variables as well. Here, we show that a refined subselection procedure that accounts both for the NAO index and for the three additional modes of sea level pressure variability, is able to further increase the prediction skill of wintertime mean sea level pressure, near-surface temperature and precipitation across Europe.

Plain Language Summary

Atmospheric winter conditions in Europe are primarily controlled by the varying pressure field over the North Atlantic, inducing generally cold/mild and dry/wet weather in Europe. Current seasonal forecasts of European winter climate, though highly desirable for society and economy, are as yet not fully reliable. There exist a number of autumn predictors, such as sea surface and stratospheric temperature, Eurasian snow depth, and Arctic sea ice, that impact on the upcoming pressure regimes in a predictable way. The present dynamical seasonal forecast systems respond still too weakly to these known seasonal predictors. But the relationship is reproduced quite well by means of statistics. In combination, statistical and dynamical forecasts have the potential to improve forecasts of the North Atlantic pressure conditions and thereby affected variables like temperature and precipitation in Europe considerably. We extend an existing hybrid seasonal forecast procedure by considering more modes of variability of the Atlantic pressure regimes than just the North Atlantic Oscillation. In this way, we are able to improve the forecasts for temperature and precipitation over wider regions in Europe.

1 Introduction

Seasonal prediction is a field of active research with several meteorological institutions worldwide issuing such seasonal forecasts to support environmental and economic decisions of a wide range of user groups. To date, the greatest success of such dynamical

44 ical ensemble forecast systems is the prediction of ENSO (El Niño Southern Oscillation)
45 several months ahead, which is the most important mode of interannual variability of
46 the global climate influencing atmospheric phenomena around the world. In general, the
47 skill of seasonal forecasts is satisfactory in the tropics, whereas prediction of northern
48 mid-latitude seasonal climate remains challenging, as recently evaluated by Baker, Shaf-
49 frey, Sutton, et al. (2018). They show that the anomaly correlation coefficient (ACC)
50 used to measure the prediction skill of mean sea level pressure (SLP) in a multi-model
51 ensemble is low and not significant over most of the North Atlantic-European sector in
52 most of the analyzed models.

53 Cohen et al. (2019) argue that new statistical techniques can increase the accuracy
54 of seasonal forecasts and advocate the development of hybrid dynamical-statistical fore-
55 casts to produce more robust seasonal predictions. Hybrid forecasts based on circula-
56 tion specification were presented for example by Baker, Shaffrey, and Scaife (2018) and
57 Dobrynin et al. (2018).

58 In boreal winter, European weather and climate is dominated by the zonal prop-
59 agation of planetary and synoptic-scale waves. This large scale circulation is an extremely
60 high-dimensional phenomenon in real space. The technique of Principal Component Anal-
61 ysis (PCA), applied to the evolving sea level pressure (SLP) field, is one way to describe
62 the states of this phenomenon in a sparse manner. The first principal component (PC)
63 of SLP corresponds closely to the North Atlantic Oscillation (NAO) index, the impor-
64 tance of which for wintertime temperature, wind and precipitation anomalies in the North
65 Atlantic-European sector has been known for long time (J. W. Hurrell, 1995; J. Hurrell
66 et al., 2003; Thompson et al., 2003). However, despite its importance, it would be mis-
67 leading to consider the NAO in isolation. Although PCs are orthogonal by construction,
68 the components are interwoven nonlinearly, and every PC represents just one aspect of
69 the whole circulation.

70 We therefore extend our notion of SLP variability considering three further modes
71 of variability (2nd, 3rd and 4th PC) in addition to the NAO index. These modes, hence
72 called circulation indices, correspond to the Scandinavian Index (SCAN), the East At-
73 lantic/West Russian (EA/WR) and the East Atlantic (EA) pattern (although the de-
74 nomination differs between authors, (Barnston & Livezey, 1987)). Together these indices

75 explain about 80% of SLP variability. We set aside the inclusion of even more circula-
76 tion indices, as their identification in short time series is complicated by stochastic noise.

77 Comas-Bru and McDermott (2014) show that higher-order circulation indices mod-
78 ulate the relation between NAO and European climate by shifting the NAO dipole in
79 the South-West/North-East direction or rotating it in a clockwise/anticlockwise move-
80 ment. Moreover, Vihma et al. (2018) explore the effects of large scale atmospheric pat-
81 terns besides NAO on European winter temperatures.

82 Dobrynin et al. (2018) reported significant improvements in the seasonal predic-
83 tion of surface temperature (TAS) and precipitation (PR) over a large area mostly in
84 northern Eurasia: on the basis of an accurate prediction of the NAO index, "good" dy-
85 namical forecast members are selected from the forecast ensemble. But as the NAO in-
86 dex explains no more than 50% of the SLP variance, even a perfect prediction of the win-
87 ter NAO will not improve the seasonal prediction of temperature and precipitation be-
88 yond certain limits (Dobrynin et al., 2018). The objective of the present paper is to ex-
89 plore possible improvements facilitated by the specification of all four leading circula-
90 tion indices in the Euro-Atlantic sector (NAO, SCAN, EA/WR, EA).

91 To produce the mentioned accurate prediction of the NAO index, Dobrynin et al.
92 (2018) developed a statistical estimator of the mean winter NAO index with a correla-
93 tion of around 0.8 by taking into account autumn states of slowly varying boundary con-
94 ditions of the ocean and atmosphere: arctic sea ice thickness, sea surface temperature,
95 snow depth in Eurasia and stratospheric temperature in 100 hPa, see also Hall et al. (2017)
96 and L. Wang et al. (2017). Similarly, Iglesias et al. (2014) and Ossó et al. (2018) pre-
97 dict the seasonal evolution of the East Atlantic pattern based on sea surface tempera-
98 ture. Rust et al. (2015) identify a linear relationship between temperature in Europe and
99 several circulation indices, which allows the isochronic prediction of temperature anoma-
100 lies given those indices.

101 We are going to broaden the approach of Dobrynin et al. (2018) by including the
102 above mentioned predictor fields in four multiple linear regressions to predict each of the
103 four considered circulation indices. These fields have been corroborated as physically mean-
104 ingful drivers of the Euro-Atlantic SLP variability independently using causal network
105 methods by Kretschmer et al. (2016). We show that an ensemble selection technique sim-
106 ilar to Dobrynin et al. (2018), applied to the hindcasts of the operational seasonal fore-

107 cast model of the German Meteorological Service GCFS2.0, accounting for four circu-
108 lation indices, leads to substantial improvement in the forecasts of SLP, TAS and PR
109 in the North Atlantic-European sector.

110 **2 Data**

111 We use data from the operational German Climate Forecast System, version 2 (GCFS2.0).
112 GCFS2.0 is based on the MPI-ESM-HR (Müller et al., 2018; Mauritsen et al., 2018) with
113 a horizontal resolution corresponding to 0.9° in the atmosphere and an ocean resolution
114 of nominally 0.4° . In cooperation, Universität Hamburg (UHH), Max Planck Institute
115 for Meteorology (MPI) and Deutscher Wetterdienst (DWD) have developed the seasonal
116 prediction system GCFS, issuing operational seasonal forecasts once a month since 2016,
117 starting on the first day of each month covering the upcoming 6 months. The first month
118 is discarded as spin up.

119 The forecasts (both restrospective and real-time) are initialized with the state of
120 the climate system inferred from the assimilation run using a continuous full-field nudg-
121 ing for ocean, sea-ice and atmosphere (Baehr et al., 2015). ERA-Interim vorticity, di-
122 vergence, temperature and sea level pressure are used for the atmosphere, ORAS5 sea-
123 ice, temperature and salinity are used for the ocean and sea-ice model. In order to ac-
124 count for uncertainties in initial conditions, an ensemble is established consisting of 50
125 members.

126 For each of the twelve forecasts per year, a hindcast data set (retrospective fore-
127 casts) consisting of 30 members per start date is provided to derive the model climate,
128 error metrics and skill scores. In GCFS2.0, hindcast data cover the monthly starting dates
129 from 1990 through 2017. The present study concentrates on hindcasts starting in Novem-
130 ber, which is when the upcoming boreal winter (December, January, February; DJF) is
131 routinely forecasted.

132 As a complement to the assimilation run of the GCFS2.0 seasonal forecast system,
133 we will also need the assimilation of the decadal prediction system developed in the MiK-
134 lip project (Pohlmann et al., 2019) because it extends 20 years farther into the past (1958-
135 present). This system facilitates a slightly different initialization method compared to
136 the seasonal prediction system. The atmosphere is nudged with ERA40 reanalysis full-
137 field data until 1979 and ERA-Interim reanalysis data from 1980 onwards. The ocean

138 is nudged with ORAS4 reanalysis anomalies during the whole duration (1960-present)
139 of the simulation. The sea-ice is nudged with NSIDC sea-ice concentration anomalies from
140 1980 till present.

141 **3 Methods**

142 We adopt the idea of Dobrynin et al. (2018) to predict the NAO index of the up-
143 coming winter (DJF) based on four predictors, autumn sea ice thickness (SIT), snow depth
144 (SND), sea surface temperature (SST), and stratospheric temperature at 100 hPa (TA100),
145 from the assimilation run of GCFSS2.0. The actual values of the predictors are calculated
146 as an area weighted mean of monthly grid cell values, taking into account only grid cells
147 that show a significant correlation to the NAO index. We construct a multiple linear re-
148 gression estimator for the NAO index that takes all four predictors into account simul-
149 taneously.

150 Multiple linear regression estimators for the three other circulation indices (SCAN,
151 EA/WR, EA) are constructed analogously to the NAO prediction. The literature on driv-
152 ing conditions influencing these indices is rather sparse. However, as already mentioned
153 above, the large scale circulation in the North Atlantic-European sector is a complex in-
154 teraction of many factors. Boundary fields like the chosen predictors do not impact ex-
155 clusively on one or another circulation index, but the whole system, exerting a greater
156 or lesser influence on all components. For these reasons, we use the same predictors for
157 SCAN, EW/WR and EA as are proposed for the NAO in Dobrynin et al. (2018).

158 After having predicted the four circulation indices statistically, in the second step
159 we select the “best” members from the dynamical hindcast ensemble. “Best” is defined
160 here in terms of the Euclidean distance between a dynamical hindcast member’s vector
161 of indices (see subsection 4.1) and our statistically predicted index vector. The “best”
162 members are selected to build a subensemble. The new seasonal hindcasts for SLP, TAS,
163 PR etc. are based only on the subensemble instead of the complete dynamical hindcast
164 ensemble.

165 **3.1 Predictors and Regression**

166 The dynamical seasonal hindcasts for DJF is initialized on November, 1st. We there-
167 fore take the October monthly means of SST, SND and TA100 as predictors, as this is

168 the latest information known when the integration starts. For SIT, we use the Septem-
169 ber monthly mean, because it reflects the annual minimum sea ice extension (Dobrynin
170 et al., 2018).

171 The correlation between the predictor values and the circulation indices is calcu-
172 lated on grid cell basis. Grid cells, which show a significant positive correlation, are com-
173 bined to an area weighted sum, as well as grid cells with significant negative correlation.
174 Consequently, each predictor can contribute two exogenous variables to the multi-linear
175 regression. Before entering the regression, the area weighted sums are centered and de-
176 trended.

177 The performance of the proposed estimation procedure is evaluated in subsection
178 4.2 in the so-called backtesting mode (see Supporting Information), a realistic cross val-
179 idation setting, where the prediction at a given time is based exclusively on information
180 from its past. In the backtesting mode, we find a high year-to-year variation of the re-
181 gions, where grid cells with significant correlations between SST and the circulation in-
182 dices are detected. In some cases this effect leads to a failure in the prediction of the cir-
183 culation indices. We assume that the relation between SST and the circulation indices
184 is sensitive to the length of the time series, because this effect does not occur when all
185 data is used for the detection. As a remedy, we replace the assimilation time series of
186 SST and SLP (for the calculation of circulation indices) from GCFS2.0 by the respec-
187 tive time series from the latest MiKLip assimilation, which start as early as 1958. The
188 Miklip assimilation is utilized exclusively to detect the significant grid cells. For the cal-
189 culation of the predictor values we return to the GCFS2.0 assimilation time series.

190 An ordinary least squares algorithm is performed to estimate the regression coef-
191 ficients. In order to avoid overfitting, the combination of predictor variables is selected
192 so as to minimize the Mean Squared Error (MSE) of the predicted index in the back-
193 testing mode (see Supporting Information), using a maximum of four predictors.

194 **3.2 Subselection**

195 The subselection of members from the dynamical seasonal hindcast ensemble is based
196 on the statistically predicted circulation indices. To compute the circulation indices re-
197 alized by each ensemble member, we use the principal components calculated from the
198 assimilation SLP fields. It is very probable that, when applying a PCA to the union of

199 all dynamical seasonal hindcast ensembles, the principal components will not coincide
200 with the GCFS2.0 assimilation. However, for a meaningful comparison between statis-
201 tically predicted circulation index and its counterpart in a dynamical forecast run, the
202 indices have to refer to the same principal component pattern. We therefore project the
203 dynamical forecast members onto the patterns from the assimilation.

204 We can now fix the number of circulation indices to be included in the subselec-
205 tion (only one index [NAO], or more than one up to 4). The Euclidean distance is cal-
206 culated between the index vectors of the dynamical hindcast ensemble members and the
207 vector of statistically predicted indices for a given winter. The Euclidean distance is weighted
208 by the Eigenvalues of the principal components to emphasize the importance of the re-
209 spective circulation index. Subsequently, the members with the smallest distance to the
210 statistical prediction are selected to build the subensemble. We reiterate the post pro-
211 cessing for this subensemble, like generating the ensemble mean, terciles and skill scores
212 for variables of interest like TAS and PR as we have done before on the complete ensem-
213 ble.

214 **3.3 Selection by Machine Learning Procedures**

215 Further refinements of the subselection that make use of various machine learning
216 procedures are conceivable. We would like to name but a few, details and results of which
217 are described in the Supporting Information. A most obvious refinement would be the
218 weighted mean of the hindcast members according to their proximity to the statistically
219 predicted circulation indices. More sophisticated, a clustering of the vectors of circula-
220 tion indices would allow for nonlinear interdependencies between the four circulation in-
221 dices, apart from linear orthogonality imposed by PCA. To improve the achieved strat-
222 ification of the clusters with respect to TAS (or any other selected parameter), a semi-
223 supervised clustering algorithm or a discriminant analysis could be applied.

224 **4 Results**

225 **4.1 Circulation Indices**

226 In this section, we examine our assumption that the seasonal hindcast skill ben-
227 efits from the inclusion of further circulation indices in the ensemble subselection pro-

228 cedure of Dobrynin et al. (2018). To this end, we repeat their perfect-NAO prediction
229 experiment and compare it to an analogue perfect-circulation indices experiment.

230 The assimilation run from the current seasonal forecast model GCFSS2.0 starts in
231 1980, hindcasts were provided for start dates in 1990-2017. We consider seasonal means
232 for winter (DJF), such that our time series starts in winter 1980/81 and runs through
233 winter 2017/18, a total of 38 time steps. In order to calculate the winter circulation in-
234 dices, singular value decomposition is applied to the area-weighted non-standardized anoma-
235 lies of seasonal SLP over the North Atlantic-European sector ($20-85^{\circ}\text{N}$ and $90^{\circ}\text{W}-60^{\circ}\text{E}$),
236 Figure 1. Note that the subsequent standardization of the indices does not affect our com-
237 putations.

238 Likewise, the ensemble members of the seasonal hindcast ensembles are projected
239 onto the same principal components extracted from the assimilation to calculate the re-
240 spective circulation indices.

241 Now, we select those members from the hindcast ensembles, which reproduce the
242 true circulations indices most closely – first only for the NAO index, after that for NAO,
243 SCAN, EA/WR and EA indices. The forecast skill of the full and of the two subensem-
244 bles is plotted in figure S1 in the Supporting Information.

245 The improvement in anomaly correlation coefficients (ACC) for SLP in the Euro-
246 Atlantic sector when selecting for all four indices, taken over time at each point sepa-
247 rately, is strong. In particular, the zonal band of low predictability between 50°N and
248 60°N , that stands out in the perfect NAO only ensemble, is completely recovered in the
249 four indices ensemble. The ACCs for TAS and PR show considerable improvements, too
250 (Figure S1).

251 We therefore conclude that the subselection for more than one circulation index
252 is worthwhile—as long as we are able to construct reliable predictors for them.

253 **4.2 Regression**

254 We evaluate the whole estimation and subselection procedure in the backtesting
255 mode, as this is the most realistic setting possible in view of prospective operationaliza-
256 tion (see Supporting Information), and the most challenging at the same time. In the
257 following, we will evaluate our predictions and the resulting hindcast skill against the

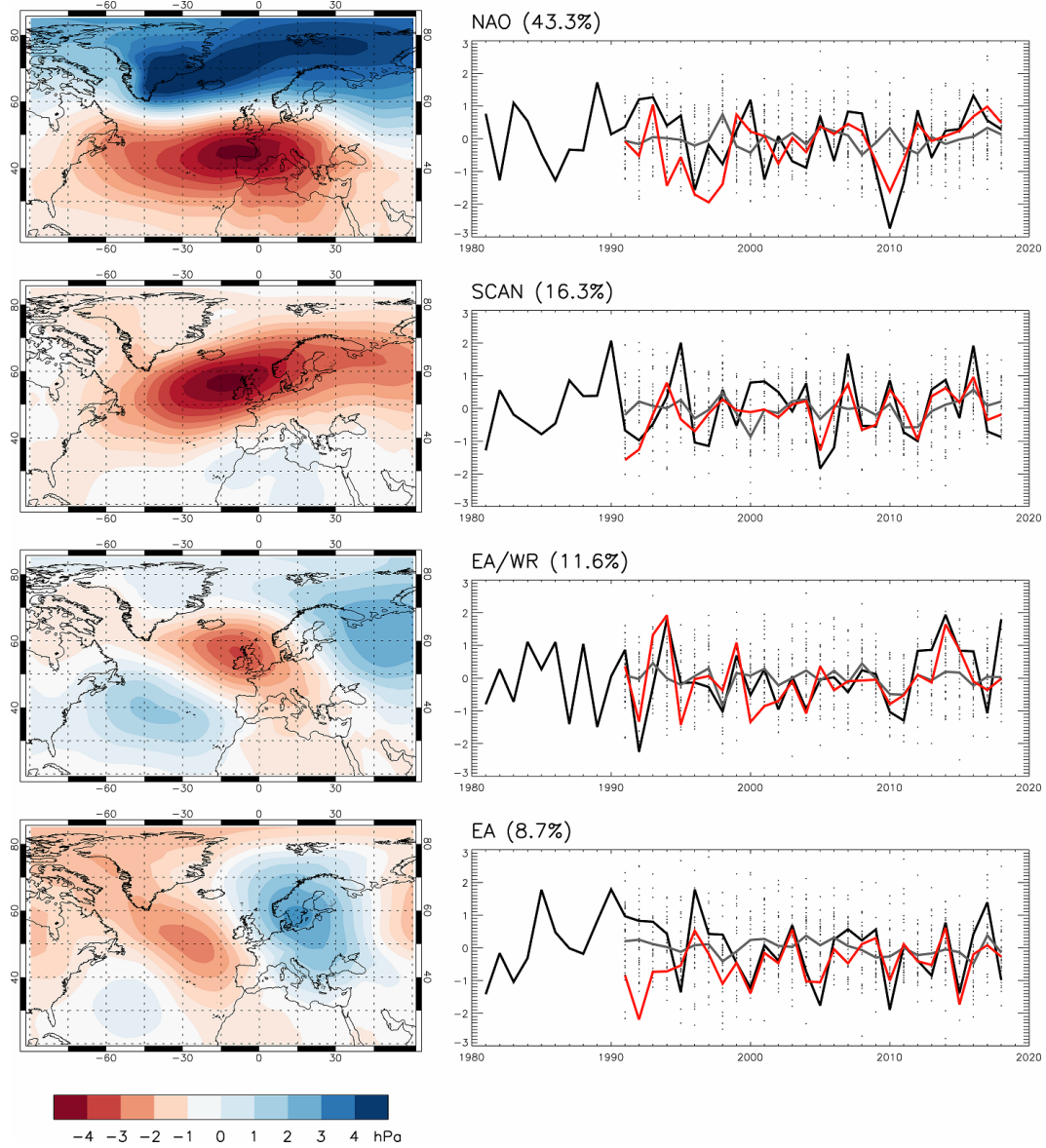


Figure 1. Circulation indices from winters 1980/81-2017/18. Left column: PC loadings for SLP anomalies. Right column: yearly winter PC scores. Black line: GCFs2.0 assimilation, grey line: ensemble mean, grey dots: ensemble members, red line: statistical prediction.

Table 1. Correlation of dynamically hindcasted and statistically predicted to assimilated circulation indices, respectively

	dyn hc	stat pr	SST	SND	SIT	TA100
NAO	0.26/0.15	0.59/0.93	+ -	-	+	
SCAN	0.35/0.56	0.66/0.88	-	-	+ -	
EA/WR	0.35/0.40	0.68/0.73	+ -	+		-
EA	0.23/0.21	0.47/0.80		+ -		+ -

Periods of correlation (DJF 1990/91-2017/18)/(DJF 2003/04-2017/18); Selected predictors: + positively correlated grid cells selected, - negatively correlated grid cells selected

258 assimilation run of GCFS2.0. We choose the assimilation run over the obvious alterna-
 259 tive ERA-Interim for the following reasons: The GCFS assimilation and ERA-Interim
 260 are both model assimilations, but the GCFS assimilation was produced with the same
 261 model as the hindcasts as opposed to ERA-Interim. The mismatch of the hindcasts will
 262 therefore be a priori smaller to the GCFS assimilation, independently of the quality of
 263 the hindcasts. Here, we aim to evaluate the relative differences in skill generated by the
 264 subselection, so for the moment we set aside model differences between GCFS and ERA-
 265 Interim.

266 The selected predictors and respective correlations between assimilated and sta-
 267 tistically predicted circulation indices (as described in subsection 3.1) are listed in Ta-
 268 ble 1, along with the correlation of the full ensemble mean indices for comparison. Both
 269 the algorithm that detects significant predictor grid cells and the least squares estima-
 270 tion are statistical procedures which need a minimum of training data to achieve a cer-
 271 tain goodness-of-fit. For early prediction times in the backtest setting, there is only a
 272 small amount of data available to train the procedures, which results in poor predictions.
 273 We observe that the correlation between the predicted indices and the assimilation strongly
 274 depends on the time interval on which the correlation is calculated, with higher values
 275 towards the end of the time period. For the purpose of illustration, we give two corre-
 276 lation values for each circulation index in Table 1, one for the winter seasons 1990/91-
 277 2017/18, the second for 2003/04-2017/18. A corresponding improvement over time is not
 278 apparent in the dynamical ensemble.

279 In the following we will solely refer to the evaluation period of winters 2003/04-2017/18
280 to highlight the potential of the proposed procedure. We note that all statistical esti-
281 mators perform quite well, see Figure 1.

282 4.3 Subselection

283 To evaluate whether the subselection leads to an improvement in the seasonal hind-
284 cast, we first analyse the anomaly correlation coefficients (ACC) between the ensemble
285 mean of the two hindcasts (subensemble vs. complete ensemble) and the GCFS2.0 as-
286 similation values. Varying the number of selected hindcasts between 4 and 20, we ob-
287 tained the highest increases in ACC for subensembles of 8 members.

288 We furthermore varied the number of circulation indices considered in the subs-
289 election. It turns out that already the inclusion of the NAO index alone greatly improves
290 the association between hindcast and assimilation (Figure 2). As expected, for the hind-
291 cast fields SLP, TAS and PR the ACC increases with each additional circulation index
292 included. The area-weighted average ACC over Europe (10°W - 30°E and 35°N - 65°N) for
293 SLP is calculated for the full ensemble/NAO-only subselection/4-indices subensemble:
294 0.24/0.63/0.73. Analogous mean ACCs for TAS amount to 0.41/0.49/0.58 and for PR
295 to 0.22/0.33/0.41.

296 4.4 Spatial Evaluation of Individual Hindcasts

297 To further explore the improvement in our temperature hindcasts obtained by sub-
298 selecting for circulation indices, we compare the individual hindcasts for winter seasons
299 2008/09, 2009/10 and 2015/16 with the respective GCFS2.0 assimilation in Figure 1. Win-
300 ters 2009/10 and 2015/16 represent distinctive atmospheric conditions showing unusual
301 values in their circulation indices (2009/10 - very low NAO and low EA, 2015/16 - high
302 NAO and very high SCAN), whereas winter 2008/09 shows average values in all four in-
303 dices. We find that the assimilation values are poorly reflected in the full ensemble mean
304 indices, except for EA/WR in 2008/09, but they are estimated well by our statistical pro-
305 cedure (Figure 1).

306 The assimilation temperature anomalies in the three selected winters are quite pro-
307 nounced. In contrast, the hindcasts anomalies for 2009/10 and 2015/16 from the full en-
308 semble appear quite pale (we concentrate on 10°W - 30°E and 35°N - 65°N , a region that

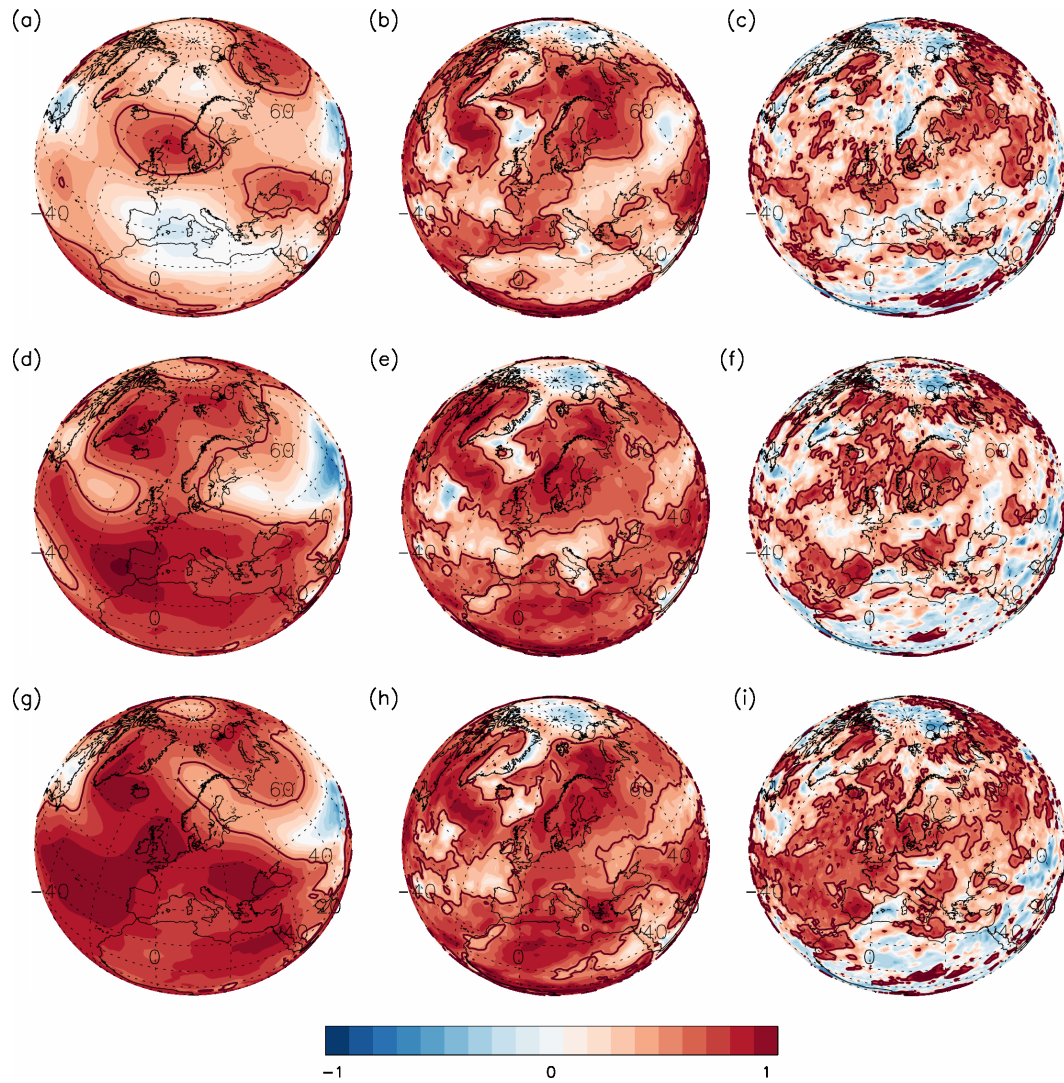


Figure 2. Anomaly correlation coefficients between hindcast ensemble means and assimilation for winters 2003/04-2017/18. 1st row: complete ensemble, 2nd row: subselection for NAO, 3rd row: subselection for NAO, SCAN, EA/WR, EA. Left column: SLP, center column: TAS, right column: PR. Regions, where the ACC is significantly positive to the 95% level (critical value 0.441), are contoured in dark red.

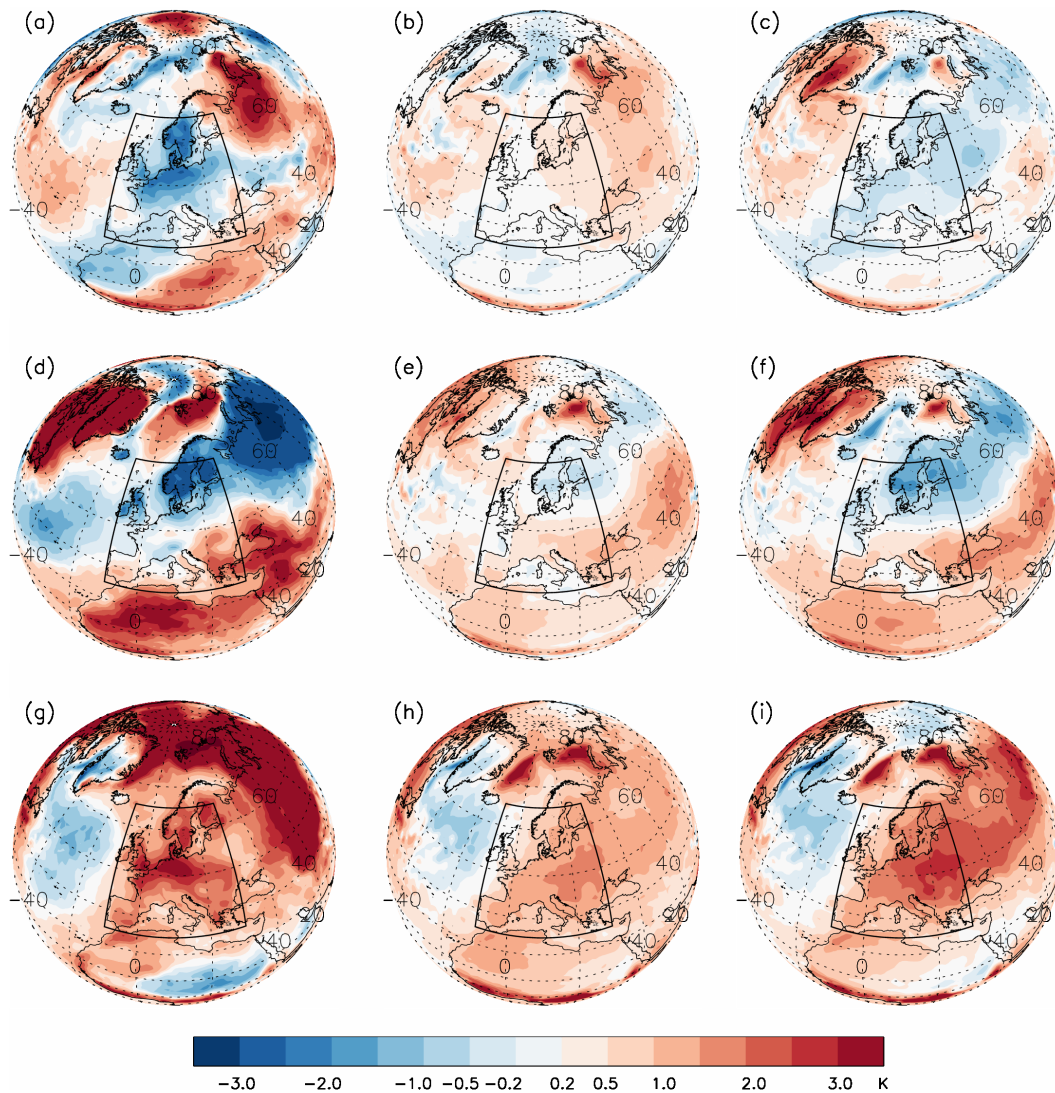


Figure 3. Temperature anomalies for 2008/09 (1st row), 2009/10 (2nd row) and 2015/16 (3rd row). Left column: GCFSS2.0 assimilation, center column: full ensemble, right column: subensemble. Black contoured rectangle: the target area 10°W - 30°E , 35°N - 65°N

309 constitutes a natural target for the German Meteorological Service, see Figure 3). For
 310 2008/09 the full ensemble mean hindcast fails completely to capture the generalized cold
 311 anomaly. After subselection, in 2009/10 the spatial pattern of anomalies is very well re-
 312 produced and also the warm hindcast anomalies for 2015/16 are increased and much closer
 313 to the analysed ones. For winter 2008/09, the subselected forecast shows a cold anomaly
 314 reversing the full ensemble hindcast. However, all subselected anomalies are still weakly
 315 pronounced in amplitude comparing to the assimilation run (Figure 3).

316 To quantify the goodness-of-fit of the individual full and subselected ensemble hind-
317 casts, we evaluate the Structural Similarity Index (SSIM) (see Supporting Information
318 and Z. Wang et al. (2004)) over the target region (Figure 3). Within this region, we weight
319 grid cell contributions to the SSIM by area. As might be suspected from visual inspec-
320 tion, SSIM between TAS hindcasts and assimilations is markedly increased by subsam-
321 pling. A further improvement is obtained by simple rescaling, which results in an am-
322 plification of both the cold and warm anomalies towards more realistic values, opening
323 prospects for more sophisticated bias correction methods (see Table S1 in the Support-
324 ing Information).

325 Although the SSIM increase by subselection with regard to TAS is most pronounced
326 in the selected years, the average skill for TAS SSIM in 2004-2018 has also more than
327 doubled (Supporting Information Table S2). For SLP and PR the increase obtained by
328 subselection is even more and slightly less pronounced, respectively. The results obtained
329 using other selection procedures (subsection 3.3), which partly surpass the improvements
330 of the simple subselection by far, are listed in the Supporting Information (Table S2).

331 5 Summery and Discussion

332 We have constructed an ensemble selection procedure based on the statistical pre-
333 diction of the four leading principal components of SLP in the North Atlantic-European
334 sector, which leads to a substantial improvement of seasonal hindcast skill for winter (DJF)
335 hindcasts of SLP, TAS and PR compared to the full ensemble mean hindcasts. This method
336 is evaluated in the backtesting mode, with average anomaly correlation over Europe for
337 SLP, TAS and PR of 0.73, 0.58 and 0.41, respectively. The statistical predictions rely
338 solely on the autumn states of four drivers of atmospheric circulation, which are known
339 at the time the dynamical model integration starts. The procedure is therefore fully ap-
340 plicable to operational forecasts.

341 The presented subsampling method is tailored to improve the seasonal hindcasts
342 in winter over Europe, only. Skill over other regions and seasons is thus possibly degraded.
343 Nonetheless, an analogue approach aiming at other regions and seasons is conceivable.

344 We have to assume that the relationships between the predictors, the circulation
345 indices and the seasonal climate that we exploit in our subselection might be subject to

346 climate variability as well as climate change. In the long run, strategies accounting for
347 such non-stationarity have to be developed.

348 **Acknowledgments**

349 The authors would like to thank Klaus Pankatz for providing the MiKlip assimilation
350 data and the corresponding description, and Johanna Baehr for valuable scientific dis-
351 cussions and comments on the manuscript. Hindcast data used for this study are avail-
352 able under [https://cds.climate.copernicus.eu/cdsapp#!/dataset/seasonal-monthly-single-](https://cds.climate.copernicus.eu/cdsapp#!/dataset/seasonal-monthly-single-levels?tab=form)
353 [levels?tab=form](https://cds.climate.copernicus.eu/cdsapp#!/dataset/seasonal-monthly-single-levels?tab=form).

354 **References**

- 355 Baehr, J., Fröhlich, K., Botzet, M., Domeisen, D. I. V., Kornbluh, L., Notz, D., . . .
 356 Müller, W. A. (2015, 5). The prediction of surface temperature in the new sea-
 357 sonal prediction system based on the mpi-esm coupled climate model. *Climate*
 358 *Dynamics*, *44*(9-10), 2723-2735. doi: 10.1007/s00382-014-2399-7
- 359 Baker, L., Shaffrey, L., & Scaife, A. (2018). Improved seasonal prediction of uk
 360 regional precipitation using atmospheric circulation. *International Journal of*
 361 *Climatology*, *38*, e437–e453.
- 362 Baker, L., Shaffrey, L., Sutton, R., Weisheimer, A., & Scaife, A. (2018). An in-
 363 tercomparison of skill and overconfidence/underconfidence of the wintertime
 364 north atlantic oscillation in multimodel seasonal forecasts. *Geophysical Re-*
 365 *search Letters*, *45*(15), 7808–7817.
- 366 Barnston, A., & Livezey, R. (1987). Classification, seasonality and persistence of
 367 low-frequency atmospheric circulation patterns. *Monthly Weather Review*,
 368 *115*(6), 1083–1126.
- 369 Cohen, J., Coumou, D., Hwang, J., Mackey, L., Orenstein, P., Tetz, S., & Tziper-
 370 man, E. (2019). S2s reboot: An argument for greater inclusion of machine
 371 learning in subseasonal to seasonal forecasts. *Wiley Interdisciplinary Reviews:*
 372 *Climate Change*, *10*(2), e00567.
- 373 Comas-Bru, L., & McDermott, F. (2014). Impacts of the ea and sca patterns on the
 374 european twentieth century nao-winter climate relationship. *Quarterly Journal*
 375 *of the Royal Meteorological Society*, *140*(679), 354–363.
- 376 Dobrynin, M., Domeisen, D., Müller, W., Pohlmann, H., & Baehr, J. . (2018). Im-
 377 proved teleconnection-based dynamical seasonal predictions of boreal winter.
 378 *Geophysical Research Letters*, *45*(8), 3605–3614.
- 379 Hall, R. J., Scaife, A. A., Hanna, E., Jones, J. M., & Erdélyi, R. (2017). Simple
 380 statistical probabilistic forecasts of the winter nao. *Weather and Forecasting*,
 381 *32*(4), 1585–1601.
- 382 Hurrell, J., Kushnir, Y., Ottersen, G., & Visbeck, M. E. (2003). *The north atlantic*
 383 *oscillation: Climatic significance and environmental impact*. Washington, DC:
 384 American Geophysical Union.
- 385 Hurrell, J. W. (1995). Decadal trends in the north atlantic oscillation: Regional tem-
 386 peratures and precipitation. *Science*, *269*(5224), 676–679.

- 387 Iglesias, I., Lorenzo, M., & Taboada, J. (2014). Seasonal predictability of the east
388 atlantic pattern from sea surface temperatures. *PLoS ONE*, *9*(1), e86439.
- 389 Kretschmer, M., Coumou, D., Donges, J., & Runge, J. (2016). Using causal effect
390 networks to analyze different arctic drivers of midlatitude winter circulation.
391 *Journal of Climate*, *29*(11), 4069-4081.
- 392 Mauritsen, T., Bader, J., Becker, T., Behrens, J., Bittner, M., Brokopf, R., ...
393 Roeckner, E. (2018). Developments in the mpi-m earth system model ver-
394 sion 1.2 (mpi-esm1.2) and its response to increasing co₂. *J. Adv. Modelling*
395 *Earth Syst. (JAMES)*, *11*, 998-1038. doi: 10.1029/2018MS001400
- 396 Müller, W. A., Jungclaus, J. H., Mauritsen, T., Baehr, J., Bittner, M., Budich,
397 R., ... Marotzke, J. (2018). A higher-resolution version of the max
398 planck institute earth system model (mpi-esm1.2-hr). *Journal of Advances*
399 *in Modeling Earth Systems*, *10*(7), 1383-1413. Retrieved from [https://](https://agupubs.onlinelibrary.wiley.com/doi/abs/10.1029/2017MS001217)
400 agupubs.onlinelibrary.wiley.com/doi/abs/10.1029/2017MS001217 doi:
401 10.1029/2017MS001217
- 402 Ossó, A., Sutton, R., Shaffrey, L., & Dong, B. (2018). Observational evidence of
403 european summer weather patterns predictable from spring. *Proceedings of the*
404 *National Academy of Sciences of the United States of America*, *115*(1), 59-63.
- 405 Pohlmann, H., Müller, W. A., Bittner, M., Hettrich, S., Modali, K., Pankatz, K., &
406 Marotzke, J. (2019). Realistic quasi-biennial oscillation variability in historical
407 and decadal hindcast simulations using cmip6 forcing. *Geophys. Res. Lett.*, *46*,
408 14118-14125.
- 409 Rust, H., Richling, A., Bissolli, P., & Ulbrich, U. (2015). Linking teleconnection pat-
410 terns to european temperature - a multiple linear regression model. *Meteorolo-*
411 *gische Zeitschrift*, *24*(4), 411-423.
- 412 Thompson, D., Lee, S., & Baldwin, M. (2003). *Atmospheric processes governing the*
413 *northern hemisphere annular mode/north atlantic oscillation* (Vol. 134).
- 414 Vihma, T., Graversen, R., Chen, L., Handorf, D., Skific, N., Francis, J., ... Over-
415 land, J. (2018). Effects of the tropospheric large-scale circulation on european
416 winter temperatures during the period of amplified arctic warming. *Interna-*
417 *tional Journal of Climatology*, *40*(1), 509-529.
- 418 Wang, L., Ting, M., & Kushner, P. (2017). A robust empirical seasonal prediction of
419 winter nao and surface climate. *Scientific Reports*, *7*(279).

420 Wang, Z., Bovik, A., Sheikh, H., & Simoncelli, E. (2004). Image quality assessment:
421 From error visibility to structural similarity. *IEEE Transactions on Image Pro-*
422 *cessing*, 13(4), 600-612.